Journal of Electrical & Electronics Engineering Research and Reviews

Academixs Open Access Publishers

Research Article

Effect of Waste Steel Fiber Length and Utilization Rate on the Flow Performance of Blast Furnace Slag 3D Printable Concrete Mixtures

Fatih Eren Akgümüş[1*], Hatice Gizem Şahin[2] and Ali Mardani[3]

Department of Civil Engineering, Bursa Uludag University, Nilufer-Bursa, Turkey

Corresponding Author:
Fatih Eren Akgümüş. Department of Civil Engineering, Bursa Uludag University, Nilufer-Bursa, Turkey.

Received Date: 26.09.2025 **Accepted Date:** 03.10.2025 **Published Date:** 12.10.2025

Abstract

Additive manufacturing has enabled the widespread adoption of 3D printable concrete (3DPC) mixtures in the construction industry due to their significant advantages over conventional methods. Compared to traditional formwork systems, 3DPC offers faster production times, reduced labor demands, improved workplace safety and enhanced design flexibility. However, the absence of coarse aggregates and the high proportion of fine materials and binders in these mixtures often result in inferior drying-shrinkage performance. Furthermore, the elevated binder content compromises their sustainability and economic viability relative to traditional concrete. To address these limitations, recent studies have explored the incorporation of fibers, pozzolanic materials, and industrial byproducts to enhance dimensional stability, ecological balance, and cost efficiency. In this study, blast furnace slag (BFS) was used as a partial replacement for cement at 0%, 25, 50 and 75% of the total binder volume to mitigate the environmental impact of 3DPC mixtures.

Additionally, straight steel fibers sourced from waste tires, with lengths of 5, 10 and 15 mm, were incorporated at volumetric ratios of 0%, 0.5% and 1% to improve drying-shrinkage resistance. A total of 27 experimental mixtures, including a control mix, were prepared with a constant water-to-binder ratio of 0.4 and a maximum aggregate particle size of 2 mm. The flow performance of these mixtures was evaluated, revealing a pronounced influence of the BFS substitution rate on flowability. It was determined that the water-reducing admixture requirement of the mixtures decreased with increasing blast furnace slag utilization ratio.

Key Words: 3D Printable Concrete, Blast Furnace Slag, Flow, Sustainability, Waste Tire Fiber

Introduction

Three-dimensional printable concrete (3DPC) technology represents an innovative additive manufacturing approach that facilitates moldless facilitates of complex structures through automated layer by layer deposition of cementitious materials. This emerging methodology has gained significant traction in the construction sector due to its transformative potential. The technology offers compelling advantages over conventional construction techniques, including accelerated production cycles, enhanced worker safety through reduced on-site hazards, optimized material utilization, and unprecedented architectural freedom in design realization [1,2]. Despite these benefits, the application of 3D printing technology in construction remains in a nascent stage of development.

A critical challenge lies in the absence of standardized protocols, as current industry practices lack established acceptance criteria or comprehensive regulatory frameworks specifically tailored for 3DPC [3]. Conventional concrete standards prove insufficient for addressing the unique rheological and mechanical requirements of 3D-printed concrete systems, necessitating the development of specialized guidelines. This knowledge gap has prompted extensive empirical research efforts aimed at optimizing both fresh-state properties (e.g., extrudability and buildability) and hardened-state performance characteristics of 3DPC mixtures [4].

Current research emphasizes that 3DPC mixtures must satisfy specific fresh-state performance criteria, which are principally categorized into three key parameters: extrudability buildability and shape stability [5-12]. A notable distinction between 3DPC and conventional high-strength concrete lies in their binder composition. While traditional mixtures typically contain 471–495 kg/m³ of cement, 3DPC mixtures require significantly higher cement contents (540–579 kg/m³), raising both economic and environmental concerns [13].

To address these challenges, researchers have investigated partial replacement of Portland cement with supplementary cementitious materials (SCMs), including fly ash, granulated blast furnace slag, silica fume, and limestone dust [14]. Although these mineral admixtures enhance workability and long-term mechanical properties, mirroring their effects in conventional concrete, they often compromise early-age strength development. Therefore, it has been stated that there are certain limitations regarding the use of mineral admixtures [15].

The escalating global consumption of plastic products has raised significant environmental concerns due to their persistent waste accumulation and ecological impacts [16]. This trend has led to generation of substantial plastic waste volumes, with improper disposal posing severe risks of environmental contamination. Notably, Torres et al. documented how the COVID-19 pandemic exacerbated this issue through the surge in disposable mask usage, further intensifying plastic pollution challenges [17]. Parallel concerns exist for the automotive sector, where widespread tire use generates millions of non-biodegradable waste tires annually [18].

In response to these sustainability challenges, innovative recycling approaches have emerged, including the incorporation of processed tire-derived fibers into fiber-reinforced concrete [19]. While existing literature extensively explores the application of waste tire fibers in conventional mixtures, a critical research gap persists regarding their utilization in 3DPC systems.

This study, investigates sustainable modifications to 3DPC mixtures through two key approaches: partial cement replacement with blast furnace slag at substitution rates of 0%, 25, 50, and 75% by weight, and incorporation of recycled waste tire fiber at volumetric fractions 0%, 0.5, and 1%. To evaluate fiber geometry effects, three distinct fiber lengths (5, 10, and 15 mm) were examined. The experimental design specifically focused on quantifying the influence of these variables on the flow performance, a critical parameter governing 3DPC printability.

Materials and Methods

Materials

The chemical, physical and mechanical properties of CEM I 42.5R Portland cement and blast furnace slag used obtained from their manufacturer are shown in Table 1.

Oxides (%)	Cement	Blast Furnace Slag	
SiO_2	18	35,5	
$Al2O_3$	4,75	12,4	
$Fe2O_3$	3,58	1,5	
CaO	63	38,9	
MgO	1,4	5,05	
Na_2O+0,658 K_2O	0,7	1,07	
SO_3	3,11	1,67	
Specific gravity	3,06	2,5	
Specific Surface Area (cm²/g)	3441	4950	
Compressive Strength (MPa)	7-day	42,8	-
	28-day	51,8	-
Pozzolanic Activity Index (%)	28-day	-	80
	90-day	-	90
Setting Time (min)	İnital	170	-
	Final	240	-

Table 1: Chemical composition, physical and mechanical properties of binder materials

Some properties of the water-reducing admixture used to ensure the required workability in 3DPC mixtures, shared by the manufacturer, are shown in Table 2.

Admixture	Density (g/cm3)	Solid Content (%)	pH	Chlorine Content (%)	Alkaline Content, Na2O (%)
Polycarboxylate-ether based high range water reducing	1,060	32	2-5	<0,1	<10

Table 2: Some properties of water-reducing admixtures

The river sand aggregates with a maximum particle size (D_{max}) of 2 mm was used. Physical characterization according to EN 1097-6 revealed the aggregates had a specific gravity of 2.54 and water absorption capacity of 0.4%. For fiber reinforcement, steel fibers obtained from recycled waste tires were incorporated at two volumetric fractions (0.5% and 1%) with three different lengths (5, 10, and 15 mm) to evaluate size-dependent effects. Some properties of the fibers used are given in Table 3. Additionally, images of the scissors and cut waste fibers used to cut the waste fibers to the appropriate length are shown in Figure 1-a and Figure 1-b, respectively.

Fiber Type	Fiber Length (mm)	Tensile Capacity (MPa)	Modulus of Elasticity (MPa)	Specific Gravity
Steel	5, 10, 15	1500	200000	7.8

Table 3: Some properties of waste steel fiber

Figure 1: (a) Used scissors and (b) cut waste fiber images

Mixing Ratios

The mixture design for 3DPC mixtures in this study incorporated the critical parameters for extrudability, buildability, and shape stability established by Şahin et al. [4]. Following their recommended methodology, extrudability was evaluated based on the mixture's ability to pass through the printing nozzle without clogging, while buildability was assessed through successful deposition of five consecutive layers without surface deformations. Mixtures meeting these criteria were further examined for shape stability, with those demonstrating values exceeding 95% deemed suitable for 3D printing applications. The water/binder ratio was kept constant at 0.40 in all mixtures. The experimental program included 28 different mixtures, comprising a control mixture and fiber-reinforced variants. Waste steel fiber were incorporated at two volumetric fractions (0.5% and 1%) and three lengths (5, 10, and 15 mm). The amount of material used in the production of 1 m3 of 3DPC mixtures is shown in Table 4. Fibrous mixtures are categorized based on the BFC utilization ratio, fiber utilization ratio, and fiber length. For example, a mixture containing no BFC and using 0.5% waste steel fiber in a 5 mm length is designated as K-0.5-0.5, while a mixture containing 25% BFC and using 1% waste

Mixture	Cement (kg/m³)	BFC (kg/m³)	Silica Fume (kg/m³)	Aggregate (kg/m³)	Fiber Usage Amount (kg/m³)	Water Reducing Admixture (kg/m³)
K	700	0	0	1211.3	0	2
25	525	143	0	1212.5	0	1.5
50	350	285.9	0	1216.1	0	0
75	175.2	395	28.9	1215.5	0	0
K-0,5-0,5	700	0	0	1198.6	39	2
K-1-0,5	700	0	0	1185.8	78	2
25-0,5-0,5	525	143	0	1199.8	39	1.5
25-1-0,5	525	143	0	1187	78	1.5
50-0,5-0,5	350	285.9	0	1203.4	39	0
50-1-0,5	350	285.9	0	1190.6	78	0
75-0,5-0,5	175.2	395	28.9	1202.8	39	0
75-1-0,5	175.2	395	28.9	1190	78	0
K-0,5-1	700	0	0	1198.6	39	2
K-1-1	700	0	0	1185.8	78	2
25-0,5-1	525	143	0	1199.8	39	1.5
25-1-1	525	143	0	1187	78	1.5
50-0,5-1	350	285.9	0	1203.4	39	0
50-1-1	350	285.9	0	1190.6	78	0
75-0,5-1	175.2	395	28.9	1202.8	39	0
75-1-1	175.2	395	28.9	1190	78	0
K-0,5-1,5	700	0	0	1198.6	39	2
K-1-1,5	700	0	0	1185.8	78	2
25-0,5-1,5	525	143	0	1199.8	39	1.5
25-1-1,5	525	143	0	1187	78	1.5

50-0,5-1,5	350	285.9	0	1203.4	39	0
50-1-1,5	350	285.9	0	1190.6	78	0
75-0,5-1,5	175.2	395	28.9	1202.8	39	0
75-1-1,5	175.2	395	28.9	1190	78	0

Table 4: Materials and mixing ratios used in 3DPC mixtures

Preparation of Mixtures and Method

The study produced 3DPC mixtures that met the essential requirements of extrudability, constructability, and shape stability. The mixing process followed a carefully designed workflow as depicted in Figure 2 and consisted of three key stages. First stage, the dry components, Portland cement, blast furnace slag, aggregate, and waste steel fiber, were thoroughly blended in a mixer at 62.5 rpm for 30 seconds to achieve uniform distribution. Next, water and necessary water-reducing admixtures were incorporated while continuing to mix at 62.5 rpm for 1 minute. Finally, the complete mixture underwent high-speed mixing at 125 rpm for 2 minutes to attain optimal homogeneity and rheological properties before being prepared for layer-by-layer compaction. This approach guaranteed consistent material properties throughout all experimental batches while maintaining the precise control needed for 3D printing applications. The three-stage mixing protocol was specifically designed to address the unique requirements of fiber-reinforced 3DPC mixtures, particularly focusing on achieving proper fiber distribution without compromising the workability essential for extrusion-based printing.

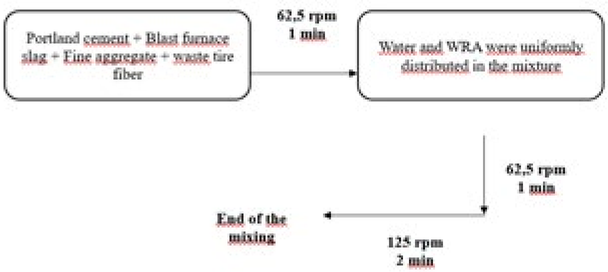

Figure 2: Preparation process of the mixtures

Flow Test

The flow value of the prepared 3DPC mixtures was made in accordance with the ASTM C1437-20 standard (Figure 3).

Figure 3: Flow test

Experimental Results and Discussion

Flow Performance

The flow values of the 3DPC mixtures produced within the scope of the study are given in Table 5. The flow performance of mixtures significantly varied depending on composition parameters. Experimental results demonstrated flow values ranging from 162.5 mm to 185 mm, with the 25-1-1.5 mixture (25% BFC, 1% 15 mm fibers) showing optimal flow characteristics and the 75-0.5-1.5 mixture (75% BFC, 0.5% 15mm fibers) exhibiting the most restricted flow. These findings align with the established printable concrete flow range of 130-210 mm reported by Zhang et al. confirming all mixtures as suitable for extrusion-based deposition [20].

A notable trend emerged regarding admixture requirements: control mixtures without BFC required 2 kg/m³ of water-reducing admixture, while BFC-containing mixtures showed reduced demand, 1.5 kg/m³ for 25% replacement and complete elimination for 50-75% replacements. This progressive decrease in chemical admixture need with increasing BFC content correlates with findings by Özbay et al. who attributed such behavior to three primary mechanisms [21].

Thermal and Hydration Effects

The lower hydration reactivity of blast furnace slag (BFS) compared to Portland cement generates less exothermic heat during initial setting [22]. This moderated thermal profile reduces early-age water evaporation, thereby maintaining mixture workability over extended periods. The slower reaction kinetics also delay stiffening, effectively extending the open time for printing operations without requiring additional water-reducing chemicals.

Particle Morphology and Lubrication

Microstructural analyses reveal that BFS particles exhibit more spherical geometries than angular cement grains [23]. This morphological advantage reduces interparticle friction within the fresh matrix, creating a ball-bearing effect that enhances flow characteristics. The resultant improvement in particle mobility diminishes the need for synthetic lubricants typically provided by conventional superplasticizers.

Surface Chemistry Interactions

With a specific surface area of 4950 cm^2/g versus cement's 3441 cm^2/g (Table 1), BFS provides greater adsorption sites for polycarboxylate-based admixtures [24]. This enhanced surface interaction promotes more efficient dispersion of cementitious particles at lower admixture dosages. The finer BFS particles also contribute to better paste phase continuity, further optimizing rheological performance through improved particle packing density.

The incorporation of silica fume (6% by volume) in mixtures with 75% BFC replacement proved essential for achieving optimal printability parameters. As demonstrated by Şahin et al. the ultra-high specific surface area (□20,000 m^2/kg) of silica fume provides two critical functions: it naturally increases the thixotropic behavior of the mixture through enhanced particle interactions, it precisely adjusts the viscosity to maintain shape stability without compromising extrudability [24]. This dual effect addresses the potential over-fluidization that could occur with high BFC content while simultaneously supporting buildability through controlled structural buildup.

Notably, the study revealed that fiber reinforcement parameters (0.5-1% volume fraction, 5-15 mm lengths) exhibited negligible influence on admixture requirements. This suggests that the dominant rheological control stems from the carefully balanced binder system (BFC-silica fume-cement ternary blend), with fiber additions primarily affecting hardened-state properties rather than fresh-state workability. The independence of admixture demand from fiber characteristics indicates that the developed matrix successfully decouples flow performance from fiber reinforcement, enabling separate optimization of printability and mechanical performance, a significant advantage for mix design flexibility in 3D concrete printing applications.

Mixture	Flow value (mm)
K	182,5
25	182,5
50	177,5
75	175
K-0,5-0,5	172,5
K-1-0,5	177,5
25-0,5-0,5	182,5
25-1-0,5	180
50-0,5-0,5	172,5
50-1-0,5	180
75-0,5-0,5	170
75-1-0,5	162,5
K-0,5-1	177,5
K-1-1	170
25-0,5-1	177,5
25-1-1	180
50-0,5-1	177,5
50-1-1	177,5
75-0,5-1	175
75-1-1	170
K-0,5-1,5	165
K-1-1,5	177,5
25-0,5-1,5	182,5
25-1-1,5	185
50-0,5-1,5	172,5
50-1-1,5	172,5
75-0,5-1,5	162,5
75-1-1,5	162,5

Table 5: Flow values of 3DPC mixtures

Results

In this study, which investigated the effect of BFC utilization ratio, fiber utilization ratio and length change on the flow value in 3DPC mixtures, the following results were obtained.

• All tested mixtures demonstrated flow values within the 162.5-185 mm range, conforming to the established printable concrete threshold of 130-210 mm reported in the literature. This consistency confirms the suitability of the developed mixtures for extrusion-based deposition processes, with optimal flow achieved in the 25% BFS-1% fiber (15mm) combination (185 mm).

• A strong inverse correlation emerged between BFS content and water-reducing admixture demand: control mixtures required 2 kg/m³, decreasing to 1.5 kg/m³ at 25% replacement, and reaching complete elimination at 50-75% BFS substitution. .

• Waste fiber characteristics (0.5-1% volume fraction, 5-15 mm lengths) showed negligible influence on fresh-state admixture requirements.

Acknowledgements

The authors would like to thank the Scientific and Technological Research Council of Turkey for supporting project number 124M212 and Bursa Uludağ University Science and Technology Center (BAP) for supporting project number FYL-2025-2130. The first author would like to thank the TÜBİTAK 2210-A program, the second author would like to thank the TÜBİTAK 2211-A program, and the third author would like to thank the Turkish Academy of Sciences (TÜBA).

References

1. Hassan, A., Alomayri, T., Noaman, M. F., & Zhang, C. (2025). 3D printed concrete for sustainable construction: A review of mechanical properties and environmental impact. Archives of Computational Methods in Engineering, 1-31.
2. Mohamed, O., Mishra, A., & Isam, F. (2025, August). An overview of 3D printed concrete for building structures: Material properties, sustainability, future opportunities, and challenges. In Structures (Vol. 78, p. 109284). Elsevier.
3. Zhang, C., Hou, Z., Chen, C., Zhang, Y., Mechtcherine, V., & Sun, Z. (2019). Design of 3D printable concrete based on the relationship between flowability of cement paste and optimum aggregate content. Cement and Concrete Composites, 104, 103406.
4. Şahin, H. G., & Mardani-Aghabaglou, A. (2022). Assessment of materials, design parameters and some properties of 3D printing concrete mixtures; a state-of-the-art review. Construction and Building Materials, 316, 125865.
5. Zhi, P., Wu, Y. C., Yang, Q., Kong, X., & Xiao, J. (2022). Effect of spiral blade geometry on 3D-printed concrete rheological properties and extrudability using discrete element modeling. Automation in Construction, 137, 104199.
6. Jayathilakage, R., Rajeev, P., & Sanjayan, J. G. (2020). Yield stress criteria to assess the buildability of 3D concrete printing. Construction and Building Materials, 240, 117989.
7. Chen, Y., Chaves Figueiredo, S., Yalçinkaya, Ç., Çopuroğlu, O., Veer, F., & Schlangen, E. (2019). The effect of viscosity-modifying admixture on the extrudability of limestone and calcined clay-based cementitious material for extrusion-based 3D concrete printing. Materials, 12(9), 1374.
8. Chen, Y., Li, Z., Chaves Figueiredo, S., Çopuroğlu, O., Veer, F., & Schlangen, E. (2019). Limestone and calcined clay-based sustainable cementitious materials for 3D concrete printing: a fundamental study of extrudability and early-age strength development. Applied Sciences, 9(9), 1809.
9. Wu, Y., Liu, C., Liu, H., Zhang, Z., He, C., Liu, S., ... & Bai, G. (2021). Study on the rheology and buildability of 3D printed concrete with recycled coarse aggregates. Journal of Building Engineering, 42, 103030.
10. Jayathilakage, R., Sanjayan, J., & Rajeev, P. (2020, July). Characterizing extrudability for 3D concrete printing using discrete element simulations. In RILEM International Conference on Concrete and Digital Fabrication (pp. 290-300). Cham: Springer International Publishing.
11. Lee, J. H., & Kim, J. H. (2022). Matric suction and its effect on the shape stability of 3D printed concrete. Cement and Concrete Research, 159, 106864.
12. Kazemian, A., Yuan, X., Meier, R., Cochran, E., & Khoshnevis, B. (2017, June). Construction-scale 3D printing: shape stability of fresh printing concrete. In International Manufacturing Science and Engineering Conference (Vol. 50732, p. V002T01A011). American Society of Mechanical Engineers.
13. Khan, S. A., Koç, M., & Al-Ghamdi, S. G. (2021). Sustainability assessment, potentials and challenges of 3D printed concrete structures: A systematic review for built environmental applications. Journal of Cleaner Production, 303, 127027.
14. Ma, G., & Wang, L. (2018). A critical review of preparation design and workability measurement of concrete material for largescale 3D printing. Frontiers of Structural and Civil Engineering, 12(3), 382-400.
15. Marchon, D., Kawashima, S., Bessaies-Bey, H., Mantellato, S., & Ng, S. (2018). Hydration and rheology control of concrete for digital fabrication: Potential admixtures and cement chemistry. Cement and concrete research, 112, 96-110.
16. Björkner, B., Frick-Engfeldt, M., Pontén, A., & Zimerson, E. (2011). Plastic materials. Contact dermatitis, 695-728.
17. Torres, F. G., & De-la-Torre, G. E. (2021). Face mask waste generation and management during the COVID-19 pandemic: An overview and the Peruvian case. Science of the Total Environment, 786, 147628.
18. Li, G., Garrick, G., Eggers, J., Abadie, C., Stubblefield, M. A., & Pang, S. S. (2004). Waste tire fiber modified concrete. Composites Part B: Engineering, 35(4), 305-312.
19. Yıldırım, Z. B., Karacasu, M., & Okur, D. V. (2018). Atık lastik ve cam lif ile modifiye edilmiş bitümün asfalt betonu performansına etkileri. Afyon Kocatepe Üniversitesi Fen ve Mühendislik Bilimleri Dergisi, 18(3), 1019-1027.
20. Zhang, C., Nerella, V. N., Krishna, A., Wang, S., Zhang, Y., Mechtcherine, V., & Banthia, N. (2021). Mix design concepts for 3D printable concrete: A review. Cement and Concrete Composites, 122, 104155.
21. Özbay, E., Erdemir, M., & Durmuş, H. İ. (2016). Utilization and efficiency of ground granulated blast furnace slag on concrete properties–A review. Construction and Building Materials, 105, 423-434.
22. Park, C. K., Noh, M. H., & Park, T. H. (2005). Rheological properties of cementitious materials containing mineral admixtures. Cement and concrete research, 35(5), 842-849.

23. He, T., Li, Z., Zhao, S., Zhao, X., & Qu, X. (2021). Study on the particle morphology, powder characteristics and hydration activity of blast furnace slag prepared by different grinding methods. Construction and Building Materials, 270, 121445.
24. Şahin, H. G., Mardani, A., & Beytekin, H. E. (2024). Effect of silica fume utilization on structural build-up, mechanical and dimensional stability performance of fiber-reinforced 3D printable concrete. Polymers, 16(4), 556.

Citation: Fatih Eren Akgümüş, Hatice Gizem Şahin and Ali Mardani, et al. (2025). Effect of Waste Steel Fiber Length and Utilization Rate on the Flow Performance of Blast Furnace Slag 3D Printable Concrete Mixtures. *J. Electr. Electron. Eng. Res. Rev.*. *1*(1), 1-7.